click for updates

ChemComm

Accepted Manuscript

Volume 1 | Number 1 | Jan 2013 | Pages 1–100

ChemComm

Chemical Communications
www.rsc.org/chemcomm

ROYAL SOCIETY OF CHEMISTRY

This is an *Accepted Manuscript*, which has been through the Royal Society of Chemistry peer review process and has been accepted for publication.

Accepted Manuscripts are published online shortly after acceptance, before technical editing, formatting and proof reading. Using this free service, authors can make their results available to the community, in citable form, before we publish the edited article. We will replace this *Accepted Manuscript* with the edited and formatted *Advance Article* as soon as it is available.

You can find more information about *Accepted Manuscripts* in the **Information for Authors**.

Please note that technical editing may introduce minor changes to the text and/or graphics, which may alter content. The journal's standard **Terms & Conditions** and the **Ethical guidelines** still apply. In no event shall the Royal Society of Chemistry be held responsible for any errors or omissions in this *Accepted Manuscript* or any consequences arising from the use of any information it contains.

ROYAL SOCIETY OF CHEMISTRY

www.rsc.org/chemcomm

ROYAL SOCIETY OF CHEMISTRY

Journal Name

ARTICLE

Functional Porous Composites by Blending with Solution-Processable Molecular Pores

S. Jiang,[a] L. Chen,[a] M. E. Briggs,[a] T. Hasell,[a] and A. I. Cooper*[a]

We present a simple method for rendering non-porous materials porous by solution co-processing with organic cage molecules. This method can be used both for small functional molecules and for polymers, thus creating porous composites by molecular blending, rather than the more traditional approach of supporting functional molecules on pre-frabricated porous supports.

Porous molecular materials have attracted considerable recent attention as gas storage materials and as sensors and separation media.[1-6] For example, porous organic cages (POCs) have been used for the separation of xylene isomers[7] and also noble gases (*e.g.*, Kr and Xe) and chiral molecules.[8] Compared to porous networks, the most distinguishing feature of 'porous molecules', such as POCs, is their solubility in common organic solvents. For example, this allows porous membranes or thin films to be cast directly from solution.[9] Solution processability also allows POCs to be combined in a 'mix and match' assembly strategy to make binary and ternary co-crystals, or to be blended with polymers to form organic-organic mixed matrix membrane (MMM) composites.[10, 11] Recently, it was shown that porous organic cages can be used as an effective catalyst support for Rh or Pd nanoparticles.[12, 13] Here, the soluble cage molecules acted as a stabiliser for the metal nanoparticles, allowed an Rh or Pd catalyst to be homogenized and leading to enhanced catalytic performance. Cage molecules might also be used as support materials for molecular catalysts or other functional molecules. Indeed, solution-processable molecular pores such as POCs could in principle underpin a wide range of functional porous composites. One challenge here is to avoid phase separation of the individual components in the composite. In the case of MMMs,[10] the formation of phase-separated **CC3** crystals in the membrane was a desirable outcome. More generally, however, it would be useful to combine functional molecules,

such as molecular catalysts, within a porous molecular framework without phase separation. This could allow a wide variety of functional porous materials to be produced by simple solution co-processing, thus circumventing some of the challenges of post-synthetic modification of insoluble porous frameworks such as metal-organic frameworks or zeolites.[14]

Here we illustrate how controlled amorphisation of molecular cages allows them to be successfully blended with a range of other functional molecules to form functional porous composites, suggesting a more general strategy where POCs can be used as 'porous additives' to introduce porosity into otherwise non-porous materials.

We previously reported a series of POCs formed by the [4+6] cycloimination reaction of 1,3,5-triformylbenzene (TFB) with vicinal diamines such as 1,2-diaminoethane (EDA) (**CC1**) and (1*R*,2*R*)-1,2-diaminocyclohexane (CHDA) (**CC3**) (Fig. 1a).[3] Porosity in these materials arises when the shape persistent intrinsic cage cavities are connected through a guest-accessible pore network. The overall porosity in the material can be increased by the incorporation of extrinsic voids between cage molecules. Subtle changes to the surface functionality of these cages was shown to have a pronounced effect on their solid-state packing, and hence their porosity.[3] Previously, we demonstrated two routes to generate *amorphous* cage materials: dynamic covalent scrambling, which forms cages with mixed surface functionality, and the freeze drying of cage solutions.[15] In the first of these two routes, scrambled cage mixtures were synthesised from EDA and CHDA (Fig. 1b), to afford a distribution of cages incorporating all possible ratios of both diamines. The mixed surface functionality and regioisomers frustrate effective packing of the cage molecules, making them less likely to crystallise. These amorphous cage materials have been showed to be more porous than many other organic molecules such as calixarenes and cucurbiturils,[16, 17] due to a large increase in extrinsic pore voids caused by inefficient packing between cages (Fig. 1c). They are also much more soluble than unscrambled cages, which allowed us to prepare porous organic liquids with a high density of unoccupied cavities.[18]

[a.] *Department of Chemistry and Centre for Materials Discovery, University of Liverpool, Crown Street, Liverpool, L69 7ZD, UK. E-mail:aicooper@liv.ac.uk; Web:* http://www.liv.ac.uk/cooper-group/

Here, the enhanced solubility helps with solution co-processability. Some studies have described membrane composites via non-covalent interactions, such as cyclodextrin polymers,[19] but these materials have not been shown to exhibit measurable porosity.
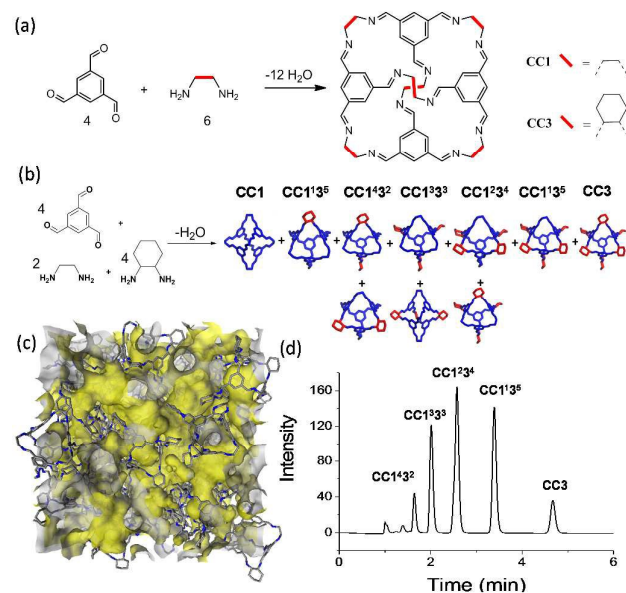

Fig. 1 (a) Synthesis of POC molecules **CC1** and **CC3**. (b) Dynamic covalent synthesis of porous scrambled organic cages (EDA : CHDA = 2 : 4). (c) The Connolly surface (yellow) was generated using a probe radius of 1.82 Å in the amorphous structural model.[13] This distribution of scrambled cages cannot pack effectively, thus creating porosity in the amorphous solid state. (d) HPLC trace showing the distribution of cage molecules in the mixture.

Scrambled cages were prepared by the co-reaction of EDA and CHDA with TFB at a molar ratio of EDA : CHDA of 2 : 4.[15] The distribution of cage molecules in the scrambled mixture, as quantified by HPLC, is shown in Fig. 1d. The resulting material is amorphous, and does not crystallize even over extended periods (90 days), and shows a high level of porosity (Brunauer-Emmett-Teller surface area, SA_{BET} = 718 m^2 g^{-1}).

Pyrene was chosen as a test molecule to blend into this scrambled porous molecular solid because its aggregation-dependent fluorescent properties allows phase separation to be detected.[20] A series of cage-pyrene composites were made by mixing different ratios of the molecular components in solution, followed by freeze-drying to remove the solvent. Powder x-ray diffraction (PXRD) showed all of the scrambled cage-pyrene composites to be amorphous, suggesting that the pyrene molecules were homogenously mixed with the scrambled cages (see Fig. S2), and that no pyrene crystallites were formed. The morphology of materials was investigated by scanning electron microscopy (SEM). Rhombohedral platelets were observed for pure pyrene (no cage), but no discernible regular crystal habit was observed for the pure scrambled cages or any of the cage-pyrene composites (Fig. S3), at least up to 16 wt.% pyrene, supporting the fact that these composite materials are amorphous. Since the cage-pyrene composites remain soluble in certain organic solvents, samples of the composite were analysed by ^{1}H NMR and this confirmed homogeneity (see Fig. S4-5). The FTIR spectra of the

POCs and pyrene did not show any significant peak shifts upon incorporation into the composites (see Fig. S6), which indicated that the pyrene molecules were mixed into the composite by relatively weak non-covalent interactions. The cage-pyrene composites were found to be fluorescent under UV light with a wavelength of 254 nm (Fig. 2a and S7), and again appeared to be homogeneous. Fluorescence spectroscopy (Fig. 2b) of composites with various pyrene-to-cage ratios showed pyrene monomer vibronic peaks at 373 nm (I1) and 383 nm (I3) and an excimer band at 470 nm. The intensity ratio between the peaks at 470 nm and 373 nm increased with increasing pyrene loading, suggesting more aggregation of the pyrene molecules in the composite at higher loadings (See Fig. S8).

The N$_2$ adsorption/desorption isotherms of cage-pyrene composites were measured at 77 K to investigate the apparent surface areas and pore volumes of the materials (Fig. 2c). All of the porous samples gave rise to Type I sorption isotherm, indicating microporosity (pores < 2 nm). Despite the non-porous nature of pure pyrene, appreciable microporosity in the composite was maintained up to around 10 wt.% pyrene loading. The amorphous scrambled cage materials exhibited a N$_2$ uptake of 11.29 mmol g^{-1} at 1 bar and 77 K, with corresponding SA_{BET} and micropore volume of 718 m^2 g^{-1} and 0.26 cm^3 g^{-1}, respectively. On introducing 3 wt.% pyrene, the N$_2$ uptake, surface area, and pore volume decreased by 12 %, as shown in Table S3. When the pyrene loading reached 16 wt.%, the saturated N$_2$ uptake drastically decreased to give a material that is effectively non-porous, at least to N$_2$ at 77 K. However, the CO$_2$ uptakes at 298 K decreased only slightly with pyrene loading, suggesting that there is dynamic porosity at higher temperatures even at high pyrene loadings. The composite containing 16 wt.% pyrene adsorbed 0.96 mmol g^{-1} CO$_2$ at 298 K and 1.0 bar, compared with 1.47 mmol g^{-1} for the pyrene-free scrambled cages. Composite materials with 3 wt.%, 6 wt.%, and 10 wt.% pyrene adsorbed 1.13, 1.32, and 1.07 mmol g^{-1} of CO$_2$, respectively (Fig. S9). Blending pyrene with scrambled cages leads to a consistent decrease in BET surface areas and N$_2$ uptakes, but only a minor loss of CO$_2$ uptakes (298 K), which suggest that pyrene is a good additive for CO$_2$ capture.[21]
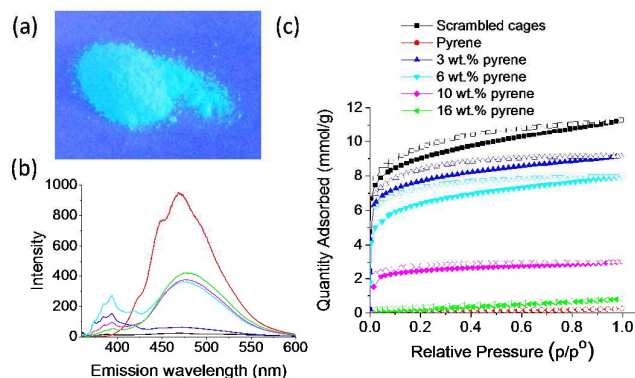

Fig. 2 (a) Photograph of a cage-pyrene composite (16 wt.% pyrene) under UV light (254 nm); (b) Fluorescence spectroscopy of pyrene and cage-pyrene composites measured in the solid state ($\lambda_{excitation}$ = 320 nm); (c) N$_2$

Journal Name | **ARTICLE**

adsorption/desorption isotherms at 77 K for the pyrene-free scrambled cage material and cage-pyrene composites with 3–16 % pyrene loading. The filled and open symbols represent adsorption and desorption, respectively.

Having established that a small molecule, pyrene, could be homogenously mixed to form porous composites, we next investigated whether porosity and homogeneity could be maintained upon blending amorphous cages with a series of non-porous polymers. The polymers tested were polyethyleneimine (PEI), polyvinylpyrrolidone (PVP), poly(methyl methacrylate) (PMMA), and polystyrene (PS). In order to screen a wide range of cage : polymer compositions, robotic dispensing and high throughput sorption screening were used. The cage-polymer composites were prepared using a robotic dispensing instrument (Eppendorf epMotion 5075PC), which allows automated liquid dispensing into sample vials. The mixed solutions were stirred on the robot deck for 1–2 h and the products were obtained by evaporating the solvents by freeze drying in parallel. Cage-polymer composites with polymer loadings ranging from 5 to 80 wt.%, were prepared and then analysed using a Quantachrome gas sorption instrument, capable of parallel 5-point BET surface area measurements over the relative pressure range 0.1–0.3. The apparent BET surface areas for the composites with various polymer loadings are shown in Fig. 3 and Fig. S10. As expected, the surface area was found to decrease with increased polymer loading for all of the composites. However, the cage-polymer composites maintained their porosity to N_2 even up to 40 wt.% polymer loading. This shows that it is possible to render non-porous commodity polymers porous simply by solution blending with soluble, molecular organic pores. Moreover, the incorporation of PEI into the composite actually *increased* the CO_2 adsorption capacity, despite decreasing the N_2-derived surface area.
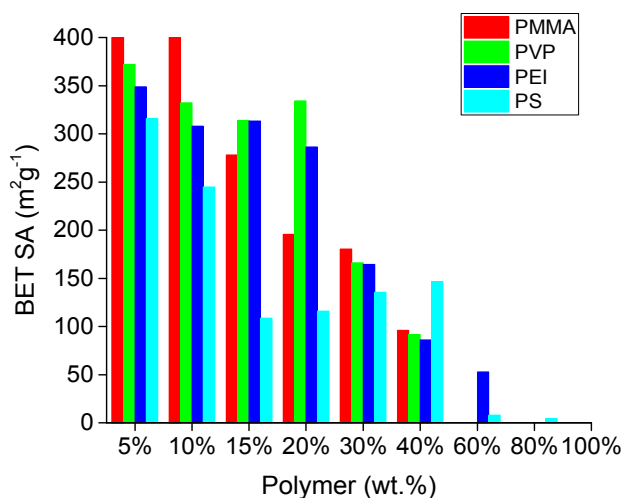

Fig. 3 SA_{BET} values for cage-polymer composites at different polymer loadings. PEI = polyethyleneimine (Mn = 5000 g mol⁻¹); PVP = polyvinylpyrrolidone (Mn = 360k g mol⁻¹); PMMA = poly(methyl methacrylate (Mn = 15k g mol⁻¹); PS = polystyrene(Mn = 192k g mol⁻¹).

Many studies on porous frameworks have shown that the incorporation of diamine or polyamine functionality can give a dramatic enhancement in CO_2 capacity and selectivity.[22-24] For example, PEI has been incorporated into porous metal-organic

frameworks (MOFs) and porous silica.[25-27] By contrast, pure, unsupported PEI is non-porous, and it exhibits only surface chemisorption. This lack of access to internal amine functionalities leads to low adsorption capacities for non-porous, bulk PEI.[28-30] Here, rather than supporting the PEI on a porous framework, we have rendered it porous by solution co-processing with a soluble molecular pore.

We carried out full characterization for the cage-PEI composites. The PEI loadings, which ranged from 5 to 33 wt.%, were verified by NMR (Fig. S11–12). The thermal stability for the cage-PEI composites was also evaluated by thermogravimetric analysis. A sharp weight loss took place at 375 °C for the cage-PEI composite, which is higher than the corresponding decomposition temperature for pure PEI. This suggests that the physical interaction of the PEI with the cage support affords greater thermal stability (Fig. S14). The composite materials are amorphous, again without any obvious phase separation, as shown by PXRD (Fig. S15).
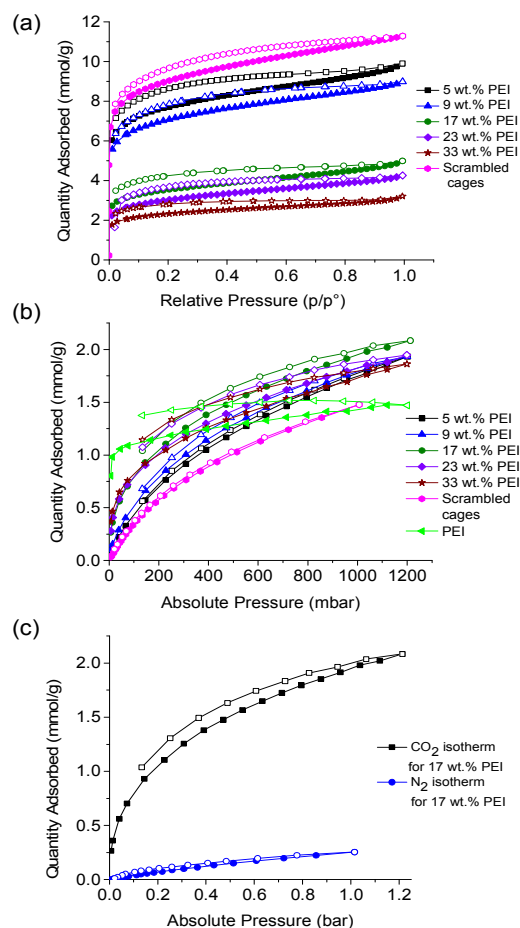

Fig. 4 (a) N_2 sorption isotherms for cage-PEI composites with different PEI loadings at 77 K. (b) CO_2 adsorption isotherms for cage-PEI composites with different PEI loading at 295 K. (c) CO_2 (black square) and N_2 (blue circle) isotherms of cage-PEI composite with 17 wt.% loading at 295 K. The filled and open symbols represent adsorption and desorption, respectively.

The N_2 sorption isotherms for the cage-PEI composites at 77 K (Fig. 4a) showed that the N_2 uptake, apparent SA_{BET} surface area, and pore volume all decreased with increased PEI loading (Table S4). As the PEI loading was increased to

33 wt.%, the N_2 uptake dropped to only 2.8 mmol g^{-1}, which indicates that the connectivity between the cage pores is reduced by the PEI. The CO_2 isotherms of the cage-PEI composites, the pure scrambled cage, and pure PEI are presented in Fig. 4b. All of the cage-PEI composites exhibited enhanced CO_2 adsorption at 1 bar compared to the pure PEI or scrambled cages, illustrating a synergistic sorption effect in the composite. At lower relative pressures, however, the PEI material absorbs more CO_2. The composite with 17 wt.% PEI loading showed the optimal CO_2 uptake at 295 K and 1 bar of 2.1 mmol g^{-1} — significantly higher than either of the pure components of the composite. The 17 wt.% PEI loading also showed an ideal CO_2/N_2 gas selectivity of 8 at 295 K and 1 bar (Fig. 4c).

Conclusions

This study shows that amorphous porous scrambled cages can be blended both with both small molecules and with polymers to form functional porous composites. There is no evidence for phase separation in the materials, and porosity is retained even with relatively high levels of the non-porous component (30–40 wt.%). This suggests a simple, solution-based processing method for forming porous composites that might have advantages over post-synthetic modification of porous frameworks — for example, in terms of processing the composites into thin films. In some cases, the functional performance of the composites can be synergistic: for example, blended composites of PEI and amorphous cages were shown to have higher CO_2 uptakes than either of the two isolated organic components. The approach also has some limitations: for example, it would be incompatible for applications involving liquid components that dissolve either the cages or the non-porous functional additive. However, we envisage a range of potential applications that involve either gases or non-solvating liquids; for example, these cages are insoluble in water and also stable under aqueous conditions.[31] This new method may be a useful route to materials such as porous polymer coatings, gas separation membranes, or materials for desalination or dialysis.

Acknowledgements

Notes and references

1. N. B. McKeown, *J. Mater. Chem.,* 2010, **20**, 10588-10597.
2. G. Zhang and M. Mastalerz, *Chem. Soc. Rev.,* 2014, **43**, 1934-1947.
3. T. Tozawa, J. T. A. Jones, S. I. Swamy, S. Jiang, D. J. Adams, S. Shakespeare, R. Clowes, D. Bradshaw, T. Hasell, S. Y. Chong, C. Tang, S. Thompson, J. Parker, A. Trewin, J. Bacsa, A. M. Z. Slawin, A. Steiner and A. I. Cooper, *Nat. Mater.,* 2009, **8**, 973-978.
4. O. Buyukcakir, Y. Seo and A. Coskun, *Chem. Mater.,* 2015, **27**, 4149-4155.
5. M. Brutschy, M. W. Schneider, M. Mastalerz and S. R. Waldvogel, *Adv. Mater.,* 2012, **24**, 6049-6052.
6. Y. Jin, B. A. Voss, R. McCaffrey, C. T. Baggett, R. D. Noble and W. Zhang, *Chem. Sci.,* 2012, **3**, 874-877.
7. T. Mitra, K. E. Jelfs, M. Schmidtmann, A. Ahmed, S. Y. Chong, D. J. Adams and A. I. Cooper, *Nat. Chem.,* 2013, **5**, 276-281.
8. L. Chen, P. S. Reiss, S. Y. Chong, D. Holden, K. E. Jelfs, T. Hasell, M. A. Little, A. Kewley, M. E. Briggs, A. Stephenson, K. M. Thomas, J. A. Armstrong, J. Bell, J. Busto, R. Noel, J. Liu, D. M. Strachan, P. K. Thallapally and A. I. Cooper, *Nat. Mater.*, 2014, **13**, 954-960.
9. Q. Song, S. Jiang, T. Hasell, M. Liu, S. Sun, A. K. Cheetham, E. Sivaniah and A. I. Cooper, *Adv. Mater.,* 2016, 28, 2629–2637.
10. A. F. Bushell, P. M. Budd, M. P. Attfield, J. T. A. Jones, T. Hasell, A. I. Cooper, P. Bernardo, F. Bazzarelli, G. Clarizia and J. C. Jansen, *Angew. Chem. Int. Ed.,* 2013, **52**, 1253-1256.
11. J. D. Evans, D. M. Huang, M. R. Hill, C. J. Sumby, A. W. Thornton and C. J. Doonan, *J. Phys. Chem. C,* 2014, **118**, 1523-1529.
12. J.-K. Sun, W.-W. Zhan, T. Akita and Q. Xu, *J. Am. Chem. Soc.,* 2015, **137**, 7063-7066.
13. B. Mondal, K. Acharyya, P. Howlader and P. S. Mukherjee, *J. Am. Chem. Soc.,* 2016, **138**, 1709–1716.
14. K. K. Tanabe and S. M. Cohen, *Chem. Soc. Rev.,* 2011, **40**, 498-519.
16. P. K. Thallapally, B. Peter McGrail, S. J. Dalgarno, H. T. Schaef, J. Tian and J. L. Atwood, *Nat. Mater.*, 2008, **7**, 146-150.
17. S. Lim, H. Kim, N. Selvapalam, K.-J. Kim, S. J. Cho, G. Seo and K. Kim, *Angew. Chem. Int. Ed.,* 2008, **47**, 3352-3355.
18. N. Giri, M. G. Del Pópolo, G. Melaugh, R. L. Greenaway, K. Rätzke, T. Koschine, L. Pison, M. F. C. Gomes, A. I. Cooper and S. L. James, *Nature*, 2015, **527**, 216-220.
19. W. Shi, L. Zhang, J. Deng, D. Wang, S. Sun, W. Zhao and C. Zhao, *J. Membr. Sci.,* 2015, **480**, 139-152.
20. J.-W. Ye, H.-L. Zhou, S.-Y. Liu, X.-N. Cheng, R.-B. Lin, X.-L. Qi, J.-P. Zhang and X.-M. Chen, *Chem. Mater.,* 2015, **27**, 8255-8260.
21. T. O. McDonald, R. Akhtar, C. H. Lau, T. Ratvijitvech, G. Cheng, R. Clowes, D. J. Adams, T. Hasell and A. I. Cooper, *J. Mater. Chem. A,* 2015, **3**, 4855-4864.
22. S. Choi, J. H. Drese and C. W. Jones, *ChemSusChem*, 2009, **2**, 796-854.
23. S. Lee, T. P. Filburn, M. Gray, J.-W. Park and H.-J. Song, *Ind. Eng. Chem. Res.,* 2008, **47**, 7419-7423.
24. D. J. Fauth, M. L. Gray, H. W. Pennline, H. M. Krutka, S. Sjostrom and A. M. Ault, *Energy Fuels*, 2012, **26**, 2483-2496.
25. Y. Lin, Q. Yan, C. Kong and L. Chen, *Sci. Rep.*, 2013, **3**, 1859-1865.
26. W.-J. Son, J.-S. Choi and W.-S. Ahn, *Microporous Mesoporous Mater.,* 2008, **113**, 31-40.
27. X. Xu, C. Song, J. M. Andresen, B. G. Miller and A. W. Scaroni, *Energy Fuels,* 2002, **16**, 1463-1469.
28. X. Ma, X. Wang and C. Song, *J. Am. Chem. Soc.,* 2009, **131**, 5777-5783.
29. N. Hiyoshi, K. Yogo and T. Yashima, *Chem. Lett.,* 2004, **33**, 510-511.
30. P. J. E. Harlick and A. Sayari, *Ind. Eng. Chem. Res.,* 2006, **45**, 3248-3255.
31. M. Liu, M. A. Little, K. E. Jelfs, J. T. A. Jones, M. Schmidtmann, S. Y. Chong, T. Hasell and A. I. Cooper, *J. Am. Chem. Soc.,* 2014, **136**, 7583-7586.

ChemComm Accepted Manuscript